Title

A genetically modulated Toll-like receptor-tolerant phenotype in peripheral blood cells of children with multisystem inflammatory syndrome.

Authors

Khan, Rehan

Ji, Weizhen

Guzman Rivera, Jeisac

et al.

Publication Date

2025-03-18

DOI

10.1093/jimmun/vkaf006

Peer reviewed

The Journal of Immunology, 2025, **214**, 373–383
https://doi.org/10.1093/jimmun/vkaf006
Advance access publication March 18, 2025
Research Article

A genetically modulated Toll-like receptor-tolerant phenotype in peripheral blood cells of children with multisystem inflammatory syndrome

Rehan Khan [1], Weizhen Ji [2], Jeisac Guzman Rivera [1], Abhilasha Madhvi [1], Tracy Andrews [3], Benjamin Richlin [4], Christian Suarez [4], Sunanda Gaur [5], Uzma N. Hasan [6], William Cuddy [7], Aalok R. Singh [7,8], Hulya Bukulmez [9], David Kaelber [9,10,11], Yukiko Kimura [12], Usha Ganapathi [1], Ioannis E. Michailidis [1], Rahul Ukey [1], Sandra Moroso-Fela [13], John K. Kuster [2], Myriam Casseus [13], Jason Roy [3], Jane C. Burns [14,15], Lawrence C. Kleinman [13,16], Daniel B. Horton [3,13,17], Saquib A. Lakhani [2], and Maria Laura Gennaro [1,18,*]

[1]Public Health Research Institute, Rutgers New Jersey Medical School, Rutgers Biomedical and Health Sciences, Newark, NJ, United States
[2]Pediatric Genomics Discovery Program, Department of Pediatrics, Yale University School of Medicine, New Haven, CT, United States
[3]Department of Biostatistics and Epidemiology, Rutgers School of Public Health, Piscataway, NJ, United States
[4]Pediatric Clinical Research Center, Rutgers Robert Wood Johnson Medical School, New Brunswick, NJ, United States
[5]Department of Pediatrics, Clinical Research Center, Rutgers Robert Wood Johnson Medical School, New Brunswick, NJ, United States
[6]Department of Pediatrics, Cooperman Barnabas Medical Center, Livingston, NJ, United States
[7]Maria Fareri Children's Hospital, Valhalla, NY, United States
[8]New York Medical College, Touro University, Valhalla, NY, United States
[9]Department of Pediatrics, Division of Rheumatology, MetroHealth System, Cleveland, OH, United States
[10]Center for Clinical Informatics Research and Education, MetroHealth System, Cleveland, OH, United States
[11]Department of Internal Medicine, Pediatrics, and Population and Quantitative Health Sciences, Case Western Reserve University, Cleveland, OH, United States
[12]Hackensack University Medical Center, Hackensack Meridian School of Medicine, Nutley, NJ, United States
[13]Department of Pediatrics, Rutgers Robert Wood Johnson Medical School, New Brunswick, NJ, United States
[14]Department of Pediatrics, University of California, San Diego, CA, United States
[15]Rady Children's Hospital-San Diego, University of California, San Diego School of Medicine, San Diego, CA, United States
[16]Department of Global Urban Health, Rutgers School of Public Health, Piscataway, NJ, United States
[17]Rutgers Center for Pharmacoepidemiology and Treatment Science, Institute for Health, Health Care Policy and Aging Research, New Brunswick, NJ, United States
[18]Department of Medicine, Rutgers New Jersey Medical School, Rutgers Biomedical and Health Sciences, Newark, NJ, United States

*Corresponding author: Maria Laura Gennaro, PHRI and Department of Medicine, Rutgers New Jersey Medical School, ICPH Building, 255 Warren Street, Newark, New Jersey 07103, United States. Email: marila.gennaro@rutgers.edu.

Abstract

Dysregulated innate immune responses contribute to multisystem inflammatory syndrome in children (MIS-C), characterized by gastrointestinal, mucocutaneous, and/or cardiovascular injury occurring weeks after severe acute respiratory syndrome coronavirus 2 (SARS-CoV-2) exposure. To investigate innate immune functions, we stimulated ex vivo peripheral blood cells from MIS-C patients with agonists of Toll-like receptors (TLR), key innate immune response initiators. We found severely dampened cytokine responses and elevated gene expression of negative regulators of TLR signaling. Increased plasma levels of zonulin, a gut leakage marker, were also detected. These effects were also observed in fully convalescent children months after MIS-C recovery. When we investigated the genetic background of patients in relation to TLR responsiveness, we found that cells from MIS-C children carrying rare heterozygous variants of lysosomal trafficking regulator (LYST) were less refractory to TLR stimulation and exhibited lysosomal and mitochondrial abnormalities with altered energy metabolism. Moreover, these rare LYST variant heterozygous carriers tended to exhibit unfavorable clinical laboratory indicators of inflammation, including more profound lymphopenia. The results of our observational study have several implications. First, TLR hyporesponsiveness may be associated with hyperinflammation and/or excessive or prolonged stimulation with gut-originated TLR ligands. Second, TLR hyporesponsiveness during MIS-C may be protective, since LYST variant heterozygous carriers exhibited reduced TLR hyporesponsiveness and unfavorable clinical laboratory indicators of inflammation. Thus, links may exist between genetic background, ability to establish a refractory immune state, and MIS-C clinical spectrum. Third, the possibility exists that prolonged TLR hyporesponsiveness is one of the mechanisms driving long coronavirus disease (COVID), which highlights the need to monitor long-term consequences of MIS-C.

Keywords: genetic variants, hyperinflammatory syndrome, innate immunity, LYST, MIS-C, SARS-CoV-2

Received: September 27, 2024. **Accepted:** January 2, 2025

Introduction

Infection with severe acute respiratory syndrome coronavirus 2 (SARS-CoV-2) is often asymptomatic or mild in children.[1–4] However, pediatric SARS-CoV-2 infection may have severe consequences. The most dramatic one is a rare syndrome with multiorgan involvement that manifests several weeks after infection with SARS-CoV-2. This clinical entity, named multisystem inflammatory syndrome in children (MIS-C), was first reported in the United Kingdom early in the pandemic[5] and subsequently defined by the US Center for Disease Control and Prevention and the World Health Organization.[6,7] Symptoms of MIS-C include fever, rash, gastrointestinal symptoms, coagulopathy, myocardial dysfunction, and/or shock.[4,8] Underlying the clinical symptoms of MIS-C are multilineage immune activation and tissue inflammation, including increased gastrointestinal permeability, elevated circulating markers of microangiopathy, and release of troponin and natriuretic peptides, indicative of cardiac inflammation.[4,8] Among the immunological abnormalities reported for MIS-C, lymphopenia is most characteristic, as it separates MIS-C from the phenotypically similar Kawasaki disease and correlates with the degree of MIS-C severity.[4,8] Still, the mechanisms of MIS-C pathogenesis remain poorly understood.[9] Unraveling the pathophysiology of MIS-C requires a better understanding of the underlying immune dysfunctions.

Multiple immunological studies have highlighted the contribution of innate immune cells to the systemic inflammation that is characteristic of MIS-C.[4,10] For example, severe cardiomyopathy in MIS-C correlates with specific inflammatory gene signatures in monocytes and dendritic cells.[11] In addition, studies on the genetic risk factors for MIS-C overwhelmingly point to innate immune responses as key to its pathogenesis.[12–14] Our current understanding of MIS-C immunology derives from the comprehensive immunological phenotyping of peripheral blood leukocytes in their basal (ie, non-perturbed experimentally) state by transcriptomics and multiparameter flow cytometry.[15–22] Except for a few case reports,[12,13] however, studies probing innate immune cell functions in MIS-C are lacking.

To characterize innate immune responses in MIS-C, we investigated the responses triggered by engagement of Toll-like receptors (TLR). TLR are membrane proteins that bind molecules produced by pathogens or released by damaged cells and initiate downstream signaling pathways leading to the increased production of antimicrobial mediators, inflammatory cytokines, chemokines, interferons (IFNs), and co-stimulatory molecules, with subsequent development of adaptive immune responses.[23–26] We report that MIS-C is associated with dampened cytokine responses to TLR stimulation and increased expression of negative regulators of TLR signaling. These phenotypes resemble TLR tolerance, a phenomenon characterized by the inability of innate immune cells to respond to further challenge when subjected to excessive or prolonged TLR stimulation.[27,28] We also find that among the least TLR-refractory cells are those from children carrying rare variants in the lysosomal trafficking regulator (*LYST*) gene locus. LYST, a multidomain protein implicated in various aspects of vesicular trafficking, affects lysosome morphology and function.[29,30] Our work reveals a novel aspect of the innate immune response during MIS-C and points to causative mechanisms and functional requirements. It also identifies genetic determinants of the expression of this refractory state, which may help explain the severity spectrum of the clinical manifestations of MIS-C.

Materials and methods

Sex as biological variable

The study included 19 males and 14 females among MIS-C patients and 3 male and 2 female healthy controls. The slight larger number of males vs females in the MIS-C group reflects enrolment in our study; it may reflect the known greater severity of SARS-CoV-2 infection in males.[31]

Study design and population

COVID-19 Network of Networks Expanding Clinical and Translational approaches to Predict Severe Illness in Children (CONNECT to Predict SIck Children) is a multicenter prospective case-control study designed to predict children at greatest risk of severe consequences from SARS-CoV-2 infection. Eligibility criteria included:

(1) Confirmed diagnoses of MIS-C; (2) age $\leq$ 21 years at time of enrollment; and (3) not pregnant either during the qualifying illness or at the time of enrollment. Children and youth with MIS-C were classified in accordance with the 2020 U.S. Centers for Disease Control criteria:[32] (1) Positivity for current or recent SARS-CoV-2 infection by RT-PCR, serology, or antigen test, or COVID-19 exposure within 4 weeks prior to onset of symptoms; (2) a combination of the following criteria: (a) fever; (b) laboratory evidence of inflammation (e.g., elevated CRP, D-dimer, IL-6); (c) evidence of clinically severe illness requiring hospitalization with dysfunction or disorders affecting at least 2 organs: cardiac, renal, respiratory, hematologic, gastrointestinal, dermatologic, or neurological; and (3) no alternative plausible diagnosis. Healthy controls were well children (3 males and 2 females) with no preexisting chronic inflammatory illness, without an acute COVID-19 illness in the past month, serologically negative for SARS-CoV-2 infection (anti-Nucleocapsid antibodies), and no acute illness at the time of study blood sample collection.

RNA sequencing data were obtained from a study involving MIS-C patients prospectively enrolled prior to the administration of MIS-C treatment, Kawasaki Disease (KD), and febrile (non MIS-C) controls.[33] All MIS-C patients met the case definition from the Centers for Disease Control and Prevention.[32] Febrile control patients had fever for at least 3 days. Final diagnosis was obtained by PCR or viral culture and included the following infections: adenovirus ($n = 12$), Epstein Barr virus ($n = 5$), 2 metapneumovirus ($n = 2$), rhinovirus ($n = 3$), influenza ($n = 3$), parainfluenza ($n = 2$), Respiratory Syncytial virus ($n = 2$), and measles ($n = 1$). All KD subjects met the disease definition by the American Heart Association (AHA) criteria.[34] Both febrile controls and KD patients had been enrolled before the COVID-19 pandemic. Additional description of subject characteristics and enrolment process are published.[33]

Study activities and data

Participants were enrolled between June 23, 2021, and November 24, 2022. Potential participants were identified through searches of electronic health records and recruited through direct contact in clinical settings or using flyers, phone calls, or emails. Following consent, parental permission, and/or assent as appropriate, participants with MIS-C

or their parents or guardians completed a questionnaire. Clinical information (medical history, treatments, clinical laboratory results, imaging, and other diagnostic tests) was obtained through medical chart review. Peripheral blood for research purposes was collected by phlebotomy at enrollment and shipped to the study biorepository. Biological parents of participants with MIS-C were also invited to participate and provide a blood or cheek swab sample for genomic sequencing. Study data were collected and managed using REDCap electronic data capture tools hosted at Rutgers Robert Wood Johnson Medical School.[35,36] A summary of demographic characteristics and MIS-C-related clinical laboratory findings is presented in Table S1.

Study approval

All study activities were approved by the Rutgers Institutional Review Board (Pro2020002961), and all participants provided informed consent prior to engaging in study activities.

Whole blood processing

Peripheral blood mononuclear cells (PBMCs) were isolated by standard density gradient centrifugation and stored in liquid nitrogen until use. Plasma was collected and stored at −80°C until use.

Whole genome and exome sequencing and analysis

Genomic DNA was isolated from peripheral blood of MIS-C patients and sequencing was performed by Illumina next generation sequencing under a research protocol at the Yale Center for Genome Analysis (YCGA). Whole genome sequencing (WGS) was carried on 22 samples with mean coverage 35×, and whole exome sequencing (WES) was carried on 11 samples with mean coverage 65×. Whole exome was captured using IDT xGen capture kit v.2.[37,38] Paired end sequence reads were converted to FASTQ format and were aligned to the reference the human genome (GRCh37/hg19). SNVs and indels were called using an automated GATK-based pipeline scripted by YCGA with AnnoVar annotation. We filtered in the exonic or splice region rare variants (MAF $\leq$ 0.005 in gnomAD) that exhibited high quality sequence reads with pass GATK Variant Score Quality Recalibration, genotype quality score GQ $\geq$ 30, a minimum 10 total reads, and $\geq$25% alternate allele ratio. We screened the results against a panel of 623 target genes related to immune function. Truncating variants (nonsense or splicing variants and indels) and missense variants with CADD $\geq$ 20 in these genes were used for rare variant analysis.

Peripheral blood mononuclear cells (PBMC) and Toll-like receptor (TLR) stimulation

Cryopreserved PBMCs were thawed and washed in pre-warmed RPMI 1640 supplemented with 2 mM L-glutamine, 10% FBS, 100 U/ml penicillin, and 100 μg/ml streptomycin (all from Corning cellgro, Manassas, Virginia, USA) (complete RPMI). PBMCs were resuspended in complete RPMI and plated in cell culture plates with different cell densities for individual experiments accordingly. Plated cells were stimulated with lipopolysaccharide (LPS; cat. no. tlrl-peklps, InvivoGen, USA). Endotoxin-free water was used as vehicle control. Culture plates were incubated for specific time at 37 °C in a 5% CO_2 humidified atmosphere accordingly.

Quantitative gene expression analysis (Q-PCR)

Thawed and resuspended PBMCs (250K/well) were plated in cell culture plates in duplicate and stimulated with LPS (50 ng/mL) and vehicle control for 4 h. Cells were harvested and washed with PBS, and RNA was isolated using RNeasy Plus Mini Kit (cat. no. 74134, Qiagen, USA) and stored at −80°C. The total RNA was reverse transcribed into cDNA using the QuantiTect Reverse Transcription Kit (cat. no. 205311, Qiagen, USA). Transcript levels for genes listed in Table S10 were measured by q-PCR using KiCqStart® SYBR® Green qPCR ReadyMix™ (Cat. No. KCQS00, Sigma-Aldrich, USA) on LightCycler® 480 II Instrument (Roche Diagnostics, USA). GAPDH was used as internal control. Primers used in q-PCR are listed in Table S10.

Multiplex cytokine analysis

Thawed and resuspended PBMCs (50,000/well) were plated in cell culture plates in duplicate and stimulated with LPS (50 ng/ml) or endotoxin-free water (vehicle control) for 24 h. After incubation, culture supernatant was collected by centrifugation at 2,000 rpm for 5 minutes and stored at −80°C. Multiplex cytokine bead assays to measure TNF-α, IL-6, IL-1β, IL-12p40, and IL-10 were performed with culture supernatants and patient plasma samples using MILLIPLEX® Human Cytokine/Chemokine Multiplex Assay kits (cat. no. HCYTA-60K, MilliporeSigma, USA). Results were analyzed with a Luminex™ xMAP™ INTELLIFLEX System. Plasma cytokine measurements were normalized to total protein in the sample.

Zonulin ELISA

Zonulin family peptides (ZFP) levels were assayed in patient plasma samples using a commercially available ELISA kit (cat. no. 30-ZONSHU-E01, ALPCO, USA), according to manufacturer's instructions. Zonulin levels were normalized to total protein in the sample.

Flow cytometry

Thawed and resuspended PBMCs (500,000/well) were plated in cell culture plates and then stimulated with LPS (50 ng/ml) and endotoxin-free water (vehicle control) for 24 h. Cells were harvested, washed with FACS buffer, centrifuged, and resuspended and incubated with Human TruStain FcX™ (cat no. 422302, BioLegend, USA) FcR blocking solution for 15 minutes. APC anti-human CD284 (TLR4) antibody (cat. no. 312816, BioLegend, USA) was then added and incubated for 30 min at 4 °C. Cells were washed with FACS buffer, centrifuged, resuspended in FACS buffer and LIVE/DEAD™ Fixable Blue Stain (cat. no. L23105, Thermo Fisher Scientific Inc., USA), and incubated in the dark for 30 min at 4 °C. Cells were washed with FACS buffer, centrifuged, resuspended in Fixation/Permeabilization solution (Cat. No. 554714, BD Biosciences, USA), and incubated for 20 minutes at 4 °C. Cells were washed with BD Perm/Wash™ buffer and resuspended in FACS buffer. Data were acquired in a BD LSRFortessa X-20 flow cytometer (BD Biosciences, San Jose, California, USA) and analyzed with FlowJo 10.9 software (FlowJo). BD™ Cytometer Setup & Tracking beads (CS&T, BD Biosciences) were used to calibrate the flow cytometer before each experiment. A total of 100,000–200,000 events were acquired per sample. Polystyrene compensation beads (BD Biosciences) were used to calculate spectral overlap

values for each fluorochrome, according to the manufacturer's instructions.

Imaging flow cytometry

Thawed and resuspended PBMCs (500,000/well) were plated in cell culture plates and stimulated with LPS (50 ng/ml) and endotoxin-free water (vehicle control) for 24 h. Cells were harvested, washed with PBS, centrifuged, resuspended in FACS buffer with Human TruStain FcX™ (Cat No. 422302, BioLegend, USA) FcR blocking solution and incubated for 15 min. PE anti-human CD45 antibody (cat. no. 304008, BioLegend, USA) was then added and incubated for 30 minutes at 4 °C. Cells were washed with FACS buffer, centrifuged, resuspended, and incubated with BD Horizon™ Fixable Viability Stain 780 (cat. no. 565388, BD Biosciences, USA) in the dark for 30 min at 4 °C. Cells were washed with FACS buffer, centrifuged, resuspended in PBS with MitoTracker™ Red CMXRos staining dye (Cat No. M7512, Invitrogen™, USA), and incubated for 30 minutes at 37 °C in a 5% CO_2 humidified atmosphere. Cells were washed with PBS, centrifuged, resuspended in Fixation/Permeabilization solution (cat. no. 554714, BD Biosciences, USA), and incubated for 20 min at 4 °C. Cells were washed with BD Perm/Wash™ buffer, resuspended in PBS, and incubated with FITC anti-human CD107a (LAMP-1) antibody (cat. no. 328606, BioLegend, USA) for 30 min at 4 °C. Data from 5,000 to 10,000 cells were acquired with an ImageStreamXMark II imaging flow cytometer (Amnis Corporation, Seattle, Washington, USA) using 60× magnification. Image data were analyzed by IDEAS software version 6.2 (Amnis Corporation, Seattle, Washington, USA) after applying a compensation matrix.

Measurement of oxidative phosphorylation and glycolysis in PBMCs

Thawed and resuspended PBMCs (500,000/well) were plated in Seahorse culture plates and cultured for 24 h at 37 °C in a 5% CO_2 humidified atmosphere. Extracellular acidification rates (ECAR) and oxygen consumption rates (OCR) were measured in XF media (nonbuffered RPMI 1640 containing 10 mM glucose, 2 mM L-glutamine, and 1 mM sodium pyruvate) under basal conditions and in response to 1.5 μM oligomycin (ATP synthase inhibitor), and 0.5 μM Rotenone and Antimycin A (Rot/AA; inhibitors of electron transport chain) by using the Seahorse XFe24 Analyzer (Agilent Technologies), according to the manufacturer's instructions. For data normalization in each well, cells were incubated with DAPI dye after measurement of OCR and ECAR for 15 min at room temperature in dark. Plates were imaged using BioTek Cytation 5 Cell Imaging Multimode Reader (Agilent), and cell numbers per well were determined by using BioTek Gen5 Software for Imaging & Microscopy (Agilent).

Statistical analysis

Data were analyzed and visualized with GraphPad Prism version 10 and STATA 18. Categorical variables were presented as frequencies and percentages; differences across groups were tested with χ^2 or Fisher exact tests, as appropriate. Continuous variables were summarized as medians with interquartile range; normality was assessed using a Kolmogorov-Smirnov test ($P < 0.001$). As these variables were non-parametric, differences across groups were tested using a Mann-Whitney *U* test or a Kruskal Wallis test, as appropriate. Box plots were drawn to show the 25th percentile, the median, and the 75th percentile of the distribution. To highlight differences in the distribution of data across groups, the coefficient of variation was calculated from the mean and standard deviation of the distribution and inset in the plots. Significance was set as $P < 0.05$ for all tests. No data were excluded from the analysis.

Results

Dampened cytokine response to LPS stimulation of peripheral blood mononuclear cells from children with MIS-C

To assess whether innate immune functions are altered by MIS-C, we subjected peripheral blood mononuclear cells (PBMC) from 17 children with MIS-C to stimulation with *E. coli* lipopolysaccharide (LPS), which is a potent TLR4 agonist.[39] For these children, peripheral blood had been collected within 30 days after hospital admission (demographic and clinical characteristics of study participants are in Table S1). Compared with PBMC from healthy controls of pediatric age, PBMC from children with MIS-C produced much lower levels of key proinflammatory cytokines, such as TNF-α, IL-6, and IL-1β (e.g., >200-fold median decrease for TNF-α), in response to LPS stimulation (Fig. 1A for heatmap and Fig. 1B for boxplots). Similar results were obtained with IL-12p40 (Fig. 1A), which is another pro-inflammatory cytokine, and the anti-inflammatory cytokine IL-10 (Fig. S1A), which is also induced in LPS-stimulated macrophages.[40,41] The diminished cytokine response to LPS stimulation was also observed by qPCR analysis of the expression levels of corresponding proinflammatory cytokine genes (Fig. 1C for heatmap and Fig. 1D for boxplots) and for IL-10 (Fig. S1B), consistent with altered TLR signaling.[25,26] These data show that peripheral blood cells from children with MIS-C are hyporesponsive to TLR4 stimulation.

Reduced TLR responses are associated with increased gene expression of negative regulators of TLR signaling, which is independent of MIS-C treatment

The observed TLR hyporesponsiveness of MIS-C PBMC recalls TLR tolerance, a long-recognized phenomenon observed in severe conditions, such as sepsis, in which prior exposure of monocytes/macrophages to microbial products results in dampened TLR responses to re-stimulation of the same or a different TLR.[27,28] Since this type of immune tolerance has been best studied, although is not limited to, LPS (endotoxin), it is often referred to as endotoxin tolerance.[28] Decreased cytokine production in endotoxin-tolerant cells is associated with increased expression of negative regulators of TLR signaling, including Toll-interacting protein (TOLLIP), suppressor of cytokine signaling (SOCS) 1, IL-1R-associated kinase-M (IRAK-M), sterile alpha and armadillo motif-containing molecule 1 (SARM1), and SH2 domain-containing inositol 5'-phosphatase 1 (SHIP-1).[42] When we used qPCR to measure the abundance of the corresponding transcripts in PBMC from MIS-C patients, we observed that the baseline (ie unstimulated) mRNA levels of SOCS1, TOLLIP, and SHIP1 were higher in the MIS-C patient cells relative to healthy controls (the comparison for SARM1 was close to significance, $P = 0.06$) (Fig. 2A for heatmap and Fig. 2B for boxplots). Increased expression of negative

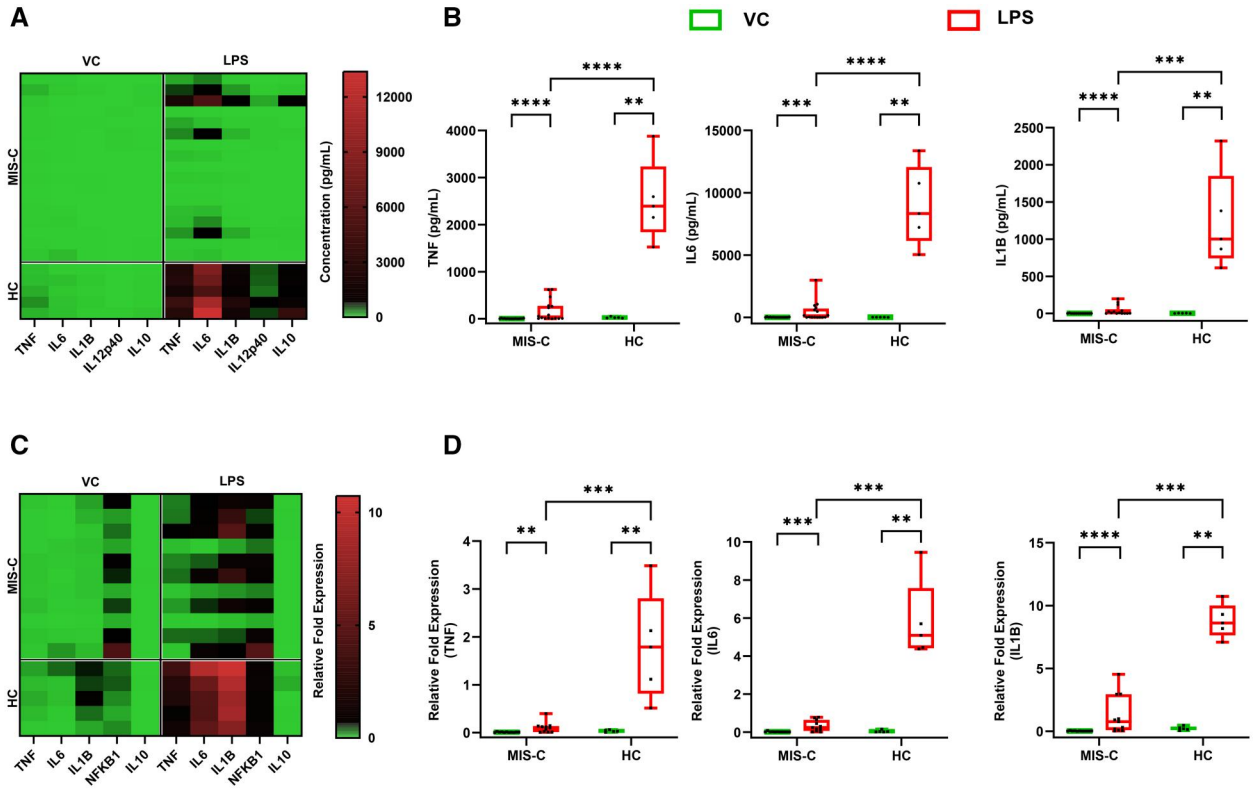

Figure 1. Cytokine production by peripheral blood mononuclear cells (PBMC) stimulated with LPS. PBMC collected from MIS-C patients within 30 days of hospital admission ($n = 17$) and from healthy controls (HC) ($n = 5$) were thawed and incubated with lipopolysaccharide (LPS, 50 ng/ml) or endotoxin-free water (vehicle control, VC); cells for RNA extraction were collected after 4 hrs of treatment; cytokine release in the culture supernatant was measured after 24 hrs of treatment. All data were generated in technical duplicates. (A, B) Cytokine release. Levels in culture supernatant was measured for several cytokines, as indicated, utilizing a Luminex® xMAP® platform and shown as heatmap, with cytokine levels in pg/ml (columns) across samples (rows), using a gradient range as shown (A). The results for three pro-inflammatory cytokines are also shown as box plots (B); additional cytokine data are shown in Fig. S1. (C, D) mRNA quantification. Expression levels of selected cytokine genes were quantified by qPCR and normalized to the control gene GAPDH. Results are shown as heatmap, with normalized gene (columns) expression levels across samples (rows) (C). mRNA levels for the corresponding inflammatory cytokines (panel B) are shown as boxplots in (D). Box plots in (B) and (D) show median value, 25th and 75th percentile, and min/max values (whiskers); black dots represent the mean of technical duplicates per study donor. *, $P < 0.05$; **, $P < 0.001$, ***, $P = 0.0001$, ****, $P < 0.0001$, ns, not significant. Mann-Whitney *U* test was used for group comparisons. HC, healthy controls; MIS-C, MIS-C patients within 30 days of hospital admission.

regulators of TLR signaling is consistent with the dampened response of MIS-C cells to TLR4 stimulation by LPS.

Children in the study were receiving treatment for MIS-C, including intravenous immunoglobulin (IVIG), at the time of blood draw. This raised the possibility of an effect of treatment on TLR responses. Through collaborations among groups funded by the NIH PreVAIL initiative on pediatric COVID-19, we had access to RNA sequencing data generated in an independent study from PBMC of MIS-C patients obtained prior to administration of any treatment and non-MIS-C controls.[33] We found that the mRNA levels for SOCS1, TOLLIP and SHIP1 were higher in the MIS-C samples than in febrile (non-MIS-C) controls (Fig. 2C). Even though the control groups differ between our study and the work of Ghosh et al.,[33] these results clearly show that the overexpression of negative regulators of TLR responses in cells from MIS-C patients cannot be explained by the treatments received by our study participants.

Kawasaki disease does not exhibit increased expression of negative regulators of TLR signaling

The Ghosh et al. study[33] also included patients with Kawasaki disease (KD), a hyperinflammatory syndrome of unknown etiology that shares many clinical features with MIS-C.[43] When we analyzed the gene expression levels of negative regulators of TLR responses in KD patients, we found that, unlike the MIS-C samples, the KD samples were indistinguishable from the febrile controls (Fig. 2C). These results suggest that TLR response downregulation is characteristic of MIS-C and identify a novel difference in pathogenesis between these 2 hyperinflammatory syndromes.

Reduced TLR responses are associated with hyperinflammation and markers of abnormal gut permeability

We reasoned that the refractory state of the innate immune cells in MIS-C patients could be explained by at least 2, non-exclusive scenarios. One relates to the excessive production of proinflammatory molecules, including cytokines, characteristic of MIS-C[4] (examples of cytokine levels in plasma of children with MIS-C are shown in Fig. 2D and Table S2). High cytokine levels might induce negative feedback mechanisms including the upregulation of negative regulators to diminish further cytokine production. This type of mechanism has been reported for SOCS1.[44] A second scenario is suggested by the finding that MIS-C is accompanied by loss of gut mucosal barrier, as indicated by the release into the

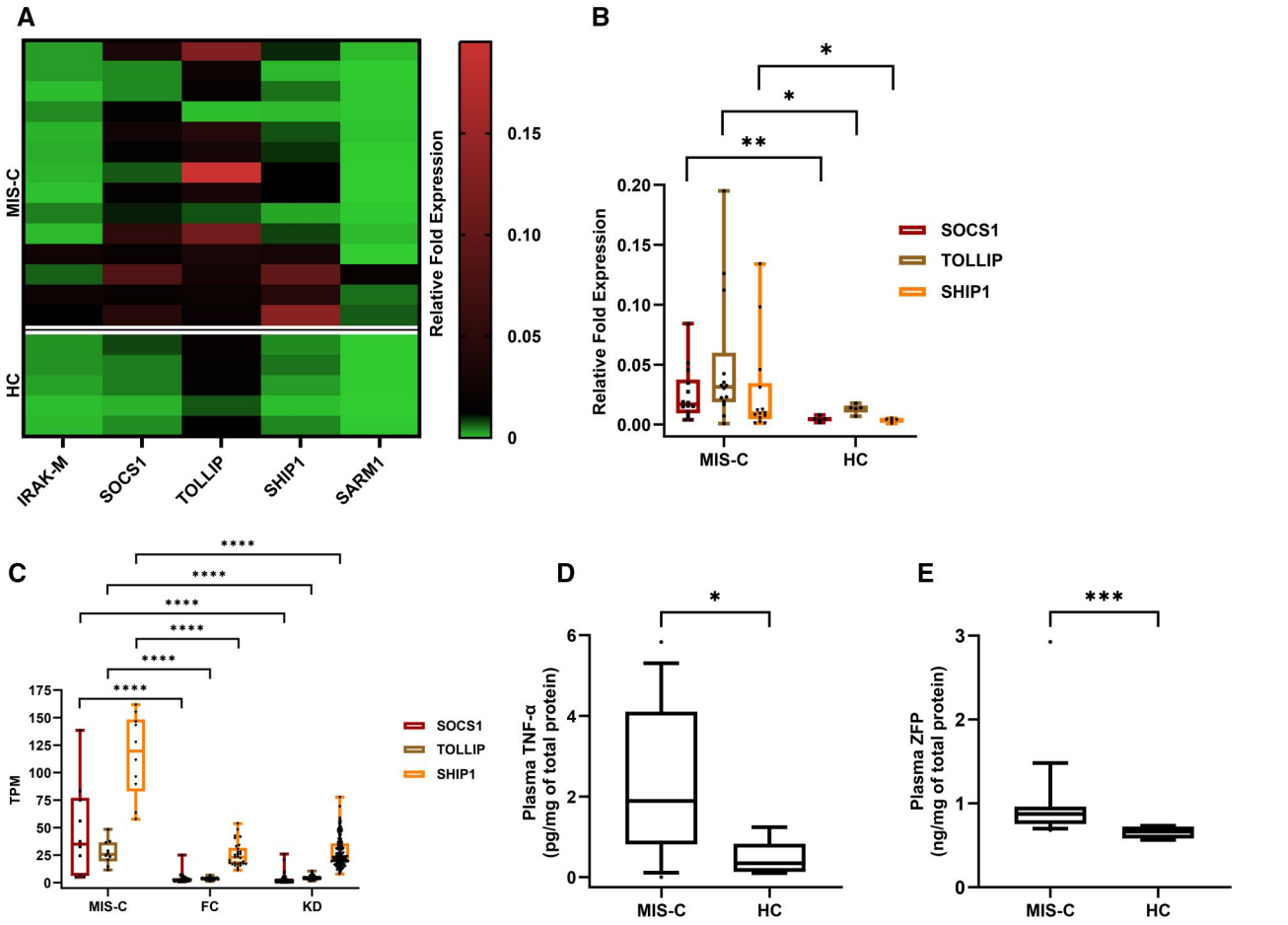

Figure 2. Mechanisms potentially responsible for TLR hypo-responsiveness. PBMC (A, B) and plasma (D, E) were obtained from peripheral blood of MIS-C patients ($n = 17$) and healthy controls (HC) ($n = 5$), as in Fig. 1. (A, B) Expression levels of genes encoding negative regulators of TLR signaling. RNA for qPCR of selected TLR signaling regulator genes was obtained from untreated PBMC collected from MIS-C patients and healthy controls (HC), as in Fig. 1. Results are shown as heatmap (A), with normalized gene (columns) expression levels across samples (rows). For selected genes, results are also shown as box plots (B), as in Fig. 1. (C) Expression levels of genes encoding negative regulators of TLR signaling by RNAseq analysis of peripheral blood cells. Whole blood was used to isolate RNA for RNA sequencing from MIS-C subjects prior to administration of treatment ($n = 10$), febrile controls (FC) ($n = 29$), and Kawasaki disease (KD) patients ($n = 136$). Both FC and KD samples were obtained prior to the COVID-19 pandemic. Cohort description is found in Methods and in.[33] Gene expression values were expressed as transcript per million (TPM) for each gene. (D) Plasma cytokine levels. The levels of major cytokines were measured in technical duplicates by utilizing a Luminex® xMAP® platform and results were normalized to total protein in the sample. (E) Plasma zonulin levels. The levels of zonulin were measured in technical duplicates by using a commercial zonulin family peptide assay kit and results were normalized to total protein in the sample, as in *Methods*. Box plots show median value, 25th and 75th percentile, and 10 to 90 percentile values (whiskers). *, $P < 0.05$; **, $P < 0.001$, ***, $P = 0.0001$, ****, $P < 0.0001$, ns, not significant (Mann-Whitney *U* test).

bloodstream of zonulin, a biomarker of intestinal permeability.[45] Consistent with this report, we found that the plasma levels of zonulin were higher in children with MIS-C, relative to healthy controls (Fig. 2E). MIS-C-induced loss of gut mucosal barrier supports the possibility that microbial products released from the gut into the bloodstream induce excessive and/or prolonged stimulation of circulating innate immune cells and consequent TLR hyporesponsiveness. Lastly, our data do not support abnormal TLR surface expression as driver of reduced TLR responsiveness, since the abundance of TLR4 on the surface of PBMC from children with MIS-C was indistinguishable from healthy controls (Fig. S2).

Reduced TLR responses and associated markers are also observed with blood samples obtained >30 days after hospital admission for MIS-C

We had available for analysis PBMC and plasma samples obtained from a group of 16 children recovered from MIS-C, for whom peripheral blood was collected more than 30 d after hospital admission (median [IQR] = 202 [81.5, 444] d) (Table S1). We were surprised to observe reduced cytokine production in response to LPS stimulation also in these fully convalescent children, relative to healthy controls (Fig. S3A). In addition, transcript levels of SOCS1, TOLLIP, SARM1, and SHIP1 (Fig. S3B) and plasma levels of zonulin (Fig. S3C) were higher in this group than in healthy controls. Together, these results suggest that TLR hyporesponsiveness and gut barrier leakage associated with MIS-C are lasting.

The cytokine response to TLR stimulation of peripheral blood mononuclear cells from children with MIS-C is not normally distributed

We compared the distribution of the cytokine data obtained in response to LPS stimulation in MIS-C and healthy control groups. We observed that the MIS-C data distribution was highly skewed, with an abundance of very low values and a tail of higher values (see the IL-6 example in Fig. 3A, left panel), unlike the normal distribution observed with the

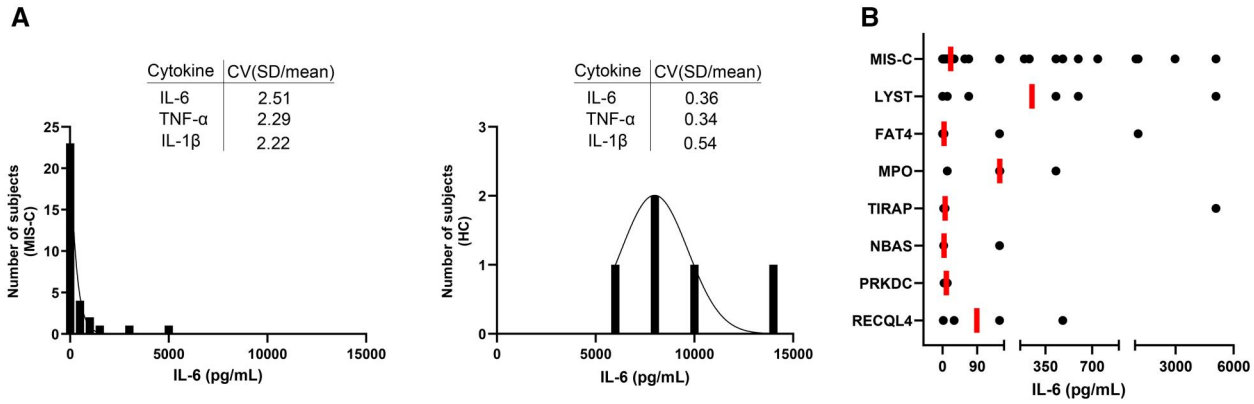

Figure 3. Distribution of cytokine release data and gene involvement. (A) Frequency distribution for IL-6 cytokine data: IL-6 cytokine levels in culture supernatants of PBMC incubated with 50 ng/ml LPS for 24 h were measured as in Fig. 1. The graph was obtained by using frequency distribution analysis and a Gaussian distribution model in GraphPad Prism; MIS-C ($n = 33$), left panel; healthy controls (HC) ($n = 5$), right panel. In both panels, the inset shows the coefficient of variation (CV) (SD/mean) for three proinflammatory cytokines. (B) Cytokine level and its distribution range in subjects with most frequently recurrent immunity-related target genes in the MIS-C group. The figure shows the distribution of data on IL-6 release from LPS-stimulated PBMC, as in (A), for all MIS-C subjects (top row) and by each of the seven most frequently recurrent immunity-related target genes among MIS-C subjects (subsequent rows, as indicated) from a list of 623 genes (Table S4). No data points are removed by the x axis breaks, which were introduced to improve data visualization. One black dot represents one donor; the vertical colored line represents the median of the distribution. The highest value in the *LYST* and *TIRAP* rows corresponds to the same donor. FAT4, FAT atypical cadherin 4; LYST, lysosomal trafficking regulator; MPO, myeloperoxidase; NBAS, NBAS subunit of NRZ tethering complex; PRKDC, protein kinase, DNA-activated subunit; RECQL4, ReqQ-like helicase; TIRAP, TIR domain containing adaptor protein.

healthy control data (Fig. 3A, right panel). The distribution differences are likely non-random, since the sample size with MIS-C in the study ($n = 33$) exceeds that of the healthy control group ($n = 5$), and samples of small sizes are less likely to be normally distributed.[46] Moreover, the positive skew of cytokine data was reflected by greater dispersion of the data (coefficients of variation, CV > 1) in the MIS-C group than in the healthy control group (CV < 1) (Fig. 3A, insets). Furthermore, the two data distributions were essentially non-overlapping: except for a single outlier, all MISC values were lower than the lowest healthy control (Fig. 3A). Thus, the 2 distributions were different in shape, dispersion, and magnitude.

Rare variants in *LYST* are associated with the skewed cytokine data distribution in MIS-C

We examined the variables underlying the data distribution in the MIS-C group. Differences in cytokine responses to TLR stimulation among children with MIS-C were not associated with demographic characteristics (such as sex at birth, age, race, or ethnicity) or time elapsed between MIS-C hospital admission and blood draw (≤ 30 d vs > 30 d) (Table S3). Thus, we next considered the genetic background of the study participants. We performed germline whole genome sequencing for children with MIS-C and analyzed the results against a list of 623 genes including Inborn Errors of Immunity genes plus additional genes having known immune function or immunodeficiency associations[47] (see Table S4). Within this gene list, we focused on rare (minor allele frequency (MAF) < 0.005) non-synonymous variants and further screened for a Combined Annotation Dependent Depletion (CADD) score of ≥ 20 to identify missense variants that were more likely to impact protein function.[48,49] We found that 7 of the 623 genes exhibited four or more non-synonymous, rare variants in the 33 MIS-C patients (Tables S5 and S6). We then examined the distribution of cytokine data in MIS-C patients grouped based on the presence of rare variants in each of these genes. We observed that the heterozygous carriers of rare non-synonymous *LYST* variants ($n = 7$) (Table S6 and Fig. S4) showed the highest median, driving the high values in the MIS-C distribution (see the IL-6 example in Fig. 3B). Moreover, the rare *LYST* variant data clustered in three groups (low, medium, and high) that mimicked those seen in the MIS-C patients. This result shows the *LYST* genotype is associated with the skewed distribution of the cytokine data in the MIS-C group.

Rare non-synonymous *LYST* variants are associated with lysosomal and mitochondrial abnormalities, altered energy metabolism, and unfavorable clinical laboratory indicators

The observed skew in the cytokine response prompted investigation of cellular phenotypes associated with rare *LYST* variants. Since LYST function has been associated with lysosome morphology and function,[29,30] we tested PBMC of rare non-synonymous *LYST* variant heterozygous carriers (Table S6) for lysosome markers. For this analysis, the similarly sized comparator group was constituted by children with MIS-C carrying common (MAF > 0.005) non-synonymous *LYST* variants (Table S7). The two subsets of children did not differ in terms of treatments received during MIS-C hospitalization or basic demographic characteristics, except for race/ethnicity (Table S8). To ensure that we were not selecting variants that were rare in the general population but common in certain racial/ethnic populations, we compared the maximum racial/ethnic subpopulation frequency of the rare *LYST* variants, which were all ≤ 0.013, versus the common variants, which were all ≥ 0.0757, indicating that our initial screen with MAF > 0.005 was appropriate. By using imaging flow cytometry, we found that the rare *LYST* variants in the MIS-C group were selectively associated with increased abundance of lysosomal-associated membrane protein 1 (LAMP1) in leukocytes (CD45+ cells) (Fig. 4A for box plots and for selected images), indicative of altered morphology and/or function of late endosomes and lysosomes in these cells.[30,50] This

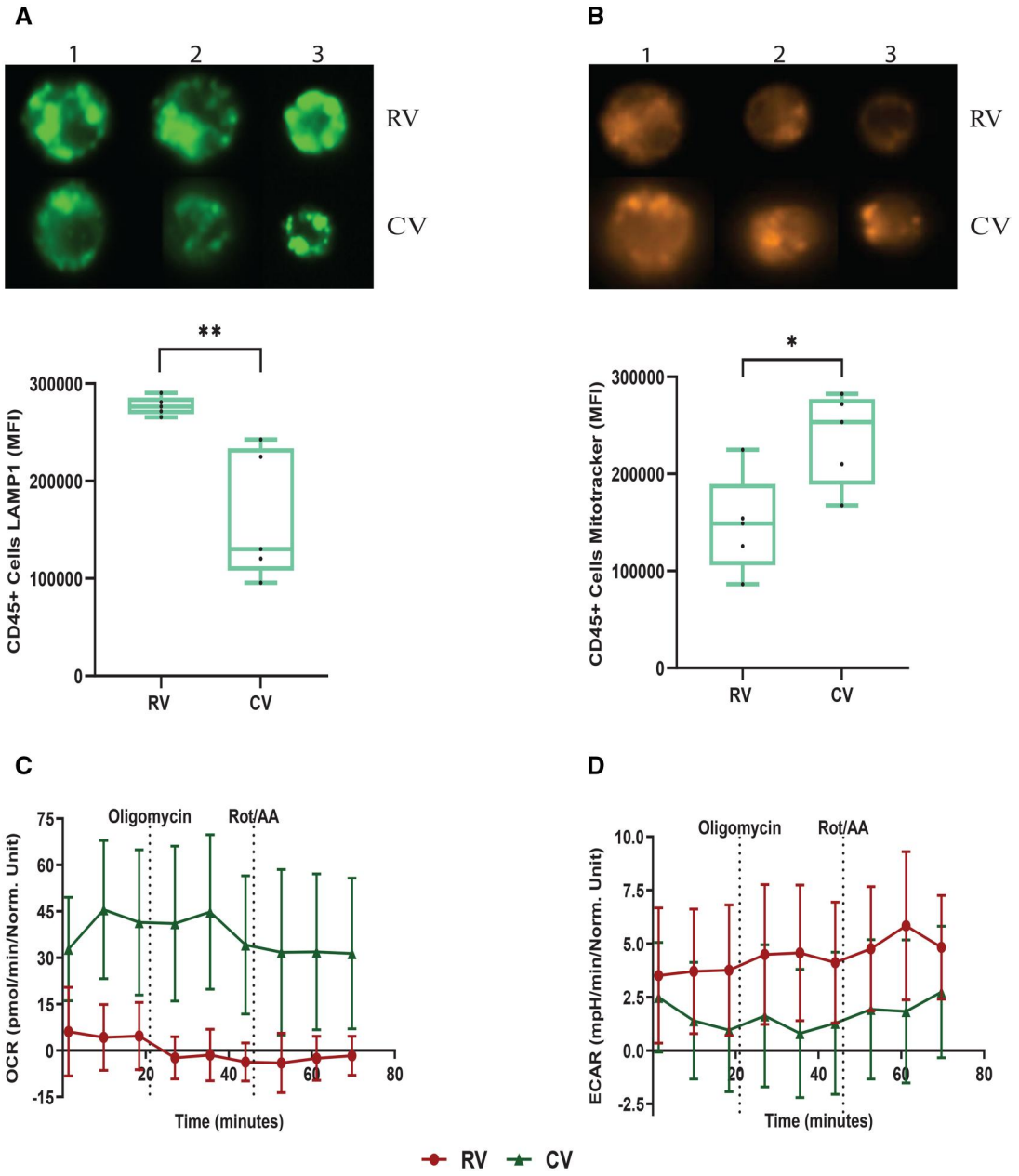

Figure 4. Analysis of lysosomal, mitochondrial, and metabolic markers associated with rare *LYST* variants. Comparisons in this figure included MIS-C subjects carrying rare *LYST* variants [minor allele frequency (MAF) < 0.005] vs MIS-C heterozygous carriers of common *LYST* variants (MAF > 0.005). RV, rare variant heterozygous carriers ($n = 5$); CV, common variant heterozygous carriers ($n = 5$ in panels AB and 4 in (C) and (D).(A, B) LAMP1 abundance (A) and MitoTracker staining (B) in CD45± cells. Data were obtained by Imaging Flow Cytometry. The figure shows representative images of three MIS-C subjects (upper panel) and box plots with median value, 25th and 75th percentile, and min/max values (whiskers) (lower panel). The relative frequency of CD45+ cells showed no significant differences between the PBMC samples from the 2 groups in the comparison. *, $P < 0.05$; **, $P < 0.001$, using Mann-Whitney *U* test.(C, D) Metabolic profile of PBMCs. Seahorse assay results for (C) oxygen consumption rates (OCR) and (D) extracellular acidification rates (ECAR) at baseline and in response to mitochondrial inhibitors. Values are presented as mean ± SEM. The unusual OCR and ECAR profiles result from person-to-person variability and data pooling—representative profiles obtained with single study subjects are shown in Fig. S5.

result is consistent with the organelle enlargement known to occur in Chediak-Higashi syndrome,[30] a rare autosomal recessive disorder that is associated with pathogenic *LYST* variants.[51,52] Lysosomal functions are intricately interconnected with mitochondrial functions,[53] which in turn shape cellular metabolism as well as immune cell functions.[54,55] Indeed, we found that the rare *LYST* variant group also exhibited decreased labeling with MitoTracker Red (Fig. 4B), a dye for active mitochondria labeling. Mitochondrial damage in the rare *LYST* variant heterozygous carriers was further indicated by reduced mitochondrial metabolism (oxidative phosphorylation) accompanied by increased non-mitochondrial metabolism (glycolysis), as measured by Seahorse XF technology (Fig. 4C and D). Collectively, the results above show that the occurrence of rare *LYST* variants is associated with altered TLR-mediated immune responses, lysosomal and mitochondrial abnormalities, and altered energy metabolism.

We next asked whether the dysfunctions observed at a cellular level in the children carrying the rare *LYST* variants

were reflected in the clinical course of MIS-C. For this assessment, we analyzed the results of laboratory tests having most relevance to MIS-C, such as markers of inflammation and white blood cell counts.[56] We observed numerical differences for key markers of disease severity between the rare and common *LYST* variant groups. White blood cell counts tended to be lower in the rare *LYST* variant group than in the common *LYST* variant counterpart. Neutrophil counts were only slightly reduced (<2-fold), but lymphopenia, which is a key finding of MIS-C,[4,56] was considerably more pronounced in the rare *LYST* variant group than in the common *LYST* variant group ($P < 0.05$). The resulting median neutrophil-to-lymphocyte ratio, which is a key marker of disease severity in many pathologies,[57] was 4-fold higher in rare than common *LYST* variant heterozygous carriers (Table S9). Despite the small size of the sample tested ($n = 13$ total across groups), the observed differences suggest that the rare *LYST* variants are associated with more severe clinical presentations.

Discussion

We report that MIS-C, the multi-system hyperinflammatory syndrome that may develop in children following exposure to SARS-CoV-2, is associated with a refractory state of the innate immune cells in the bloodstream that is evidenced as inability to respond to TLR stimulation ex vivo. TLR tolerance during MIS-C may result from the activation of negative feedback responses induced by high levels of proinflammatory mediators in the bloodstream. Increased gut permeability, as indicated by elevated plasma levels of zonulin in patients with MIS-C seen in this study and previous work,[45] might also concur to TLR tolerization by allowing microbial translocation and consequent exposure of circulating immune cells to TLR ligands of microbial origin. The detection of SARS-CoV-2 antigen, perhaps of intestinal origin,[45] in the bloodstream of MIS-C patients supports this scenario, particularly since the SARS-CoV-2 Spike glycoprotein can act as TLR ligand.[58–62] Mechanistic studies are required to test the causal associations between hyperinflammation, gut permeability, and TLR tolerance.

We also report that, among cells from children with MIS-C, the least refractory to TLR stimulation are those carrying non-synonymous, rare variants in *LYST*. This is a locus of interest in pediatric medicine and rheumatology because *LYST* variants may cause Chediak-Higashi syndrome (CHS), an autosomal recessive disorder that is characterized by easy bruising, oculocutaneous albinism, and recurrent pyogenic infections.[51,52] Pathogenic *LYST* variants and CHS are associated with risk for hyperinflammatory disorders such as MIS-C and hemophagocytic lymphohistiocytosis (HLH),[63–65] indicating links between *LYST* defects and inflammation. Moreover, a hallmark of CHS is the enlargement of late endosomes and lysosomes.[30] Thus, the altered morphology and/or function of late endosomal/lysosomal compartments observed in the *LYST* variant heterozygous carriers in our study strongly implies that *LYST* function is altered in these subjects. Furthermore, decreased mitochondrial metabolism in the *LYST* variant heterozygous carriers is consistent with lysosome regulation of mitochondrial function,[53] which shapes cellular metabolism and immune cell functions.[54,55] Mechanistic hypotheses linking *LYST* defects, organelle function, regulation of TLR activation, and inflammation will be best tested with mutant immune cell lines and animal models.

The finding that MIS-C is associated with dampened ability of innate immune cells to respond to stimulus contributes new understanding of the "post-COVID" immunological landscape. For example, it is postulated that TLR tolerance helps limit immune hyperactivation and uncontrolled inflammation, as mentioned above, but it is also associated with unfavorable outcomes, such as increased risk of secondary infections or chronic inflammatory states.[27,28] Thus, our results raise the question whether the increased incidence of infections observed in the post-COVID era could be attributed to increased susceptibility (immunity "theft") rather than to "immunity debt" from insufficient immune stimulation due to non-pharmaceutical interventions used to limit the spread of COVID-19, such as masking or social isolation.[66,67] Since MIS-C is rare among the manifestations of pediatric SARS-CoV-2 infection, addressing this question requires investigating whether other forms of pediatric COVID-19 also lead to diminished TLR responses, a possibility that our study does not exclude. Moreover, our data could help explain mechanisms of pathogenesis of post-acute sequelae of SARS-CoV-2 infection (PASC, also known as long COVID), which have affected 200 million people worldwide.[68] We were surprised to observe that PBMC obtained several months after recovery from MIS-C exhibited similar levels of TLR hyporesponsiveness as those obtained within few weeks after hospitalization for MIS-C. Our study was not designed to monitor long-term consequences of MIS-C, so we cannot exclude alternative, albeit unlikely, explanations (eg that children enrolled with MIS-C history later had unrelated conditions also associated with TLR hyporesponsiveness). It is however tempting to speculate that lasting hyporesponsiveness to TLR stimulation may result from prolonged innate immune cell stimulation. At least 2 scenarios may explain prolonged stimulus. One is viral persistence, one of the mechanisms proposed as drivers of long COVID[69] since, as mentioned above, the Spike protein of SARS-CoV-2 can act as TLR ligand.[58–62] An alternative scenario would involve the lasting, epigenetic proinflammatory reprogramming of human immune stem cells induced by SARS-CoV-2 infection,[70] since circulating innate immune cells may become tolerant in response to prolonged exposure to proinflammatory molecules. Thus, direct or indirect relationships may exist between lasting immune stimulation, innate immune tolerance, and various manifestations of long COVID.

In conclusion, our data identify TLR hyporesponsiveness as a novel immunological mechanism in MIS-C, where it may have beneficial or harmful consequences. On one hand, reduced responses to TLR stimulation may contribute to prevent runaway inflammation and protect against worse clinical outcomes. Indeed, the potential association between reduced TLR activation and unfavorable markers of inflammation observed in children with rare *LYST* variants supports a protective role of TLR hyporesponsiveness. Moreover, since MIS-C presents with varying degrees of clinical severity, child-to-child differential ability to express this refractory state and the underlying genetic determinants may help explain the severity spectrum of MIS-C manifestations. On the other hand, reduced ability to respond to TLR ligands, which may be prolonged, may result in increased post-COVID susceptibility to various infections and, potentially, contribute to long COVID. Our findings warrant further investigations to validate associations between genotypes and molecular and clinical phenotypes and to determine

whether other clinical manifestations of SARS-CoV-2 infection are also associated with TLR hyporesponsiveness. Our work also highlights the importance of longitudinal studies to monitor the health of children who have experienced MIS-C.

Acknowledgments

The authors wish to thank Karl Drlica and George Yap for critical reading of the manuscript; Rozina Aamir, Lisa Cerracchio, Wendy Dalton, Justine Griswold, Monica Konstantino, and Emanuel Lerner for their assistance with patient referral to the study, recruitment, enrollment, collection of data and biospecimens, and regulatory documentation; Mary Ellen Riordan for her insights and operational expertise in coordinating clinical sites and recruitment; the Yale Center for Genome Analysis for DNA sequencing; Charles Hevi for coordinating biospecimen collection and shipping to biorepository with consortium members; and Beth Dworetzky and Steph Lomangino from Family Voices for their assistance and guidance with recruitment materials, surveys, and other participant-facing documents. They are indebted to the MIS-C patients and their families for consenting to participate to the study.

Author contributions

Design of experimental plan (R.K., W.J., S.A.L., M.L.G.); execution of experimental work (R.K., J.G.-R., A.M., U.G., I.E. M., R.U., W.J., J.K.K.); participant recruitment, data collection, and biospecimen and data collection (B.R., C.S., S.G., W.C., A.R.S., H.B., D.K., Y.K., J.C.B.); project management (S.M.-F.); data management (M.C., D.H.); statistical analysis (T.A., J.R.); interpretation of results (all authors); manuscript writing (R.K., S.A.L., M.L.G.); critical review of manuscript (all authors); consortium leadership (M.L,G., D.H., L.C.K.).

Supplementary material

Supplementary material is available at The Journal of Immunology online.

Funding

This work was funded in part by grants by the National Institute of Child Health and Human Development HD105619, HD105593-03S2, National Institute of Allergy and Infectious Diseases R01AI158911, and National Center for Advancing Translational Sciences UM1TR004789 .

Conflicts of interest

S.A.L. is part owner of Victory Genomics and Qiyas Higher Health, two startup companies unrelated to this work. J.G.R. and M.L.G. are coinventors in provisional patent applications on MIS-C biomarkers unrelated to this work.

Data availability

All relevant data are within the manuscript and its supplementary information files. RNA sequencing data can be accessed at GSE178491. Raw data files for genomic sequencing are available upon request.

References

1. Götzinger F, et al.; ptbnet COVID-19 Study Group. COVID-19 in children and adolescents in Europe: a multinational, multicentre cohort study. Lancet Child Adolesc Health. 2020;4:653–661.
2. Viner RM et al. Susceptibility to SARS-CoV-2 infection among children and adolescents compared with adults: a systematic review and meta-analysis. JAMA Pediatr. 2021;175:143–156.
3. Tsankov BK et al. Severe COVID-19 infection and pediatric comorbidities: a systematic review and meta-analysis. Int J Infect Dis. 2021;103:246–256.
4. Chou J, Thomas PG, Randolph AG. Immunology of SARS-CoV-2 infection in children. Nat Immunol. 2022;23:177–185.
5. Riphagen S, Gomez X, Gonzalez-Martinez C, Wilkinson N, Theocharis P. Hyperinflammatory shock in children during COVID-19 pandemic. Lancet. 2020;395:1607–1608.
6. Centers for Disease Control and Prevention. Emergency preparedness and response: multisystem inflammatory syndrome in children (MIS-C) associated with coronavirus disease 2019 (COVID-19). CDC Emergency Preparedness and Response. 2021. https://emergency.cdc.gov/han/2020/han00432.asp
7. https://www.who.int/publications/i/item/multisystem-inflammatory-syndrome-in-children-and-adolescents-with-covid-19
8. Brodin P. Immune responses to SARS-CoV-2 infection and vaccination in children. Semin Immunol. 2023;69:101794.
9. Feleszko W et al.; Immunology Section and Working Group Infections of the EAACI. Pathogenesis, immunology, and immune-targeted management of the multisystem inflammatory syndrome in children (MIS-C) or pediatric inflammatory multisystem syndrome (PIMS): EAACI Position Paper. Pediatr Allergy Immunol. 2023;34:e13900.
10. Henderson LA, Yeung RSM. MIS-C: Early lessons from immune profiling. Nat Rev Rheumatol. 2021;17:75–76.
11. de Cevins C et al.; Pediatric-Biocovid Study Group. A monocyte/dendritic cell molecular signature of SARS-CoV-2-related multisystem inflammatory syndrome in children with severe myocarditis. Med. 2021;2:1072–1092.e7.
12. Lee PY et al. Immune dysregulation and multisystem inflammatory syndrome in children (MIS-C) in individuals with haploinsufficiency of SOCS1. J Allergy Clin Immunol. 2020;146:1194–1200.e1.
13. Chou J et al.; Taking on COVID-19 Together Study Investigators. Mechanisms underlying genetic susceptibility to multisystem inflammatory syndrome in children (MIS-C). J Allergy Clin Immunol. 2021;148:732–738.e1.
14. Lee D, et al.; COVID Human Genetic Effort. Inborn errors of OAS-RNase L in SARS-CoV-2-related multisystem inflammatory syndrome in children. Science. 2023;379:eabo3627.
15. Carter MJ et al. Peripheral immunophenotypes in children with multisystem inflammatory syndrome associated with SARS-CoV-2 infection. Nat Med. 2020;26:1701–1707.
16. Gruber CN et al. Mapping systemic inflammation and antibody responses in multisystem inflammatory syndrome in children (MIS-C). Cell. 2020;183:982–995.e4.
17. Lee PY et al. Distinct clinical and immunological features of SARS-CoV-2-induced multisystem inflammatory syndrome in children. J Clin Invest. 2020;130:5942–5950.
18. Sacco K et al.; Pavia Pediatric COVID-19 Group. Immunopathological signatures in multisystem inflammatory syndrome in children and pediatric COVID-19. Nat Med. 2022;28:1050–1062.
19. Vella LA et al.; UPenn COVID Processing Unit. Deep immune profiling of MIS-C demonstrates marked but transient immune activation compared to adult and pediatric COVID-19. Sci Immunol. 2021;6:eabf7570.
20. Ramaswamy A et al. Immune dysregulation and autoreactivity correlate with disease severity in SARS-CoV-2-associated multisystem inflammatory syndrome in children. Immunity. 2021;54:1083–1095.e7.
21. Consiglio CR et al.; CACTUS Study Team. The immunology of multisystem inflammatory syndrome in children with COVID-19. Cell. 2020;183:968–981.e7.

22. Diorio C et al. Multisystem inflammatory syndrome in children and COVID-19 are distinct presentations of SARS-CoV-2. J Clin Invest. 2020;130:5967–5975.
23. Kawai T, Akira S. The role of pattern-recognition receptors in innate immunity: update on Toll-like receptors. Nat Immunol. 2010; 11:373–384.
24. Kagan JC, Barton GM. Emerging principles governing signal transduction by pattern-recognition receptors. Cold Spring Harb Perspect Biol. 2014;7:a016253.
25. Kawai T, Akira S. TLR signaling. Semin Immunol. 2007;19:24–32.
26. Kawai T, Akira S. Signaling to NF-kappaB by Toll-like receptors. Trends Mol Med. 2007;13:460–469.
27. Medvedev AE, Sabroe I, Hasday JD, Vogel SN. Tolerance to microbial TLR ligands: molecular mechanisms and relevance to disease. J Endotoxin Res. 2006;12:133–150.
28. Biswas SK, Lopez-Collazo E. Endotoxin tolerance: new mechanisms, molecules and clinical significance. Trends Immunol. 2009;30:475–487.
29. Windhorst DB, Zelickson AS, Good RA. Chediak-Higashi syndrome: hereditary gigantism of cytoplasmic organelles. Science. 1966;151:81–83.
30. Burkhardt JK, Wiebel FA, Hester S, Argon Y. The giant organelles in beige and Chediak-Higashi fibroblasts are derived from late endosomes and mature lysosomes. J Exp Med. 1993;178:1845–1856.
31. Rajamanickam A et al. Sex-specific differences in systemic immune responses in MIS-C children. Sci Rep. 2024;14:1720–1730.
32. https://www.cdc.gov/mis/mis-c/hcp_cstecdc/
33. Ghosh P et al.; Pediatric Emergency Medicine Kawasaki Disease Research Group. An Artificial Intelligence-guided signature reveals the shared host immune response in MIS-C and Kawasaki disease. Nat Commun. 2022;13:2687–2704.
34. McCrindle BW et al.; American Heart Association Rheumatic Fever, Endocarditis, and Kawasaki Disease Committee of the Council on Cardiovascular Disease in the Young; Council on Cardiovascular and Stroke Nursing; Council on Cardiovascular Surgery and Anesthesia; and Council on Epidemiology and Prevention. Diagnosis, treatment, and long-term management of Kawasaki disease: a scientific statement for health professionals from the American Heart Association. Circulation. 2017;135:e927–e999.
35. Harris PA et al. Research electronic data capture (REDCap)—a metadata-driven methodology and workflow process for providing translational research informatics support. J Biomed Inform. 2009;42:377–381.
36. Harris PA et al.; REDCap Consortium. The REDCap consortium: building an international community of software platform partners. J Biomed Inform. 2019;95:103208.
37. McKenna A et al. The Genome Analysis Toolkit: a MapReduce framework for analyzing next-generation DNA sequencing data. Genome Res. 2010;20:1297–1303.
38. Wang K, Li M, Hakonarson H. ANNOVAR: functional annotation of genetic variants from high-throughput sequencing data. Nucleic Acids Res. 2010;38:e164–e170.
39. Poltorak A et al. Defective LPS signaling in C3H/HeJ and C57BL/10ScCr mice: mutations in Tlr4 gene. Science. 1998;282:2085–2088.
40. Chanteux H, Guisset AC, Pilette C, Sibille Y. LPS induces IL-10 production by human alveolar macrophages via MAPKinases- and Sp1-dependent mechanisms. Respir Res. 2007;8:71–80.
41. Chang EY, Guo B, Doyle SE, Cheng G. Cutting edge: involvement of the type I IFN production and signaling pathway in lipopolysaccharide-induced IL-10 production. J Immunol. 2007;178:6705–6709.
42. Piao W et al. Endotoxin tolerance dysregulates MyD88- and Toll/IL-1R domain-containing adapter inducing IFN-beta-dependent pathways and increases expression of negative regulators of TLR signaling. J Leukoc Biol. 2009;86:863–875.
43. Sharma C et al. Multisystem inflammatory syndrome in children and Kawasaki disease: a critical comparison. Nat Rev Rheumatol. 2021;17:731–748.
44. Huang S et al. SOCS proteins participate in the regulation of innate immune response caused by viruses. Front Immunol. 2020; 11:558341.
45. Yonker LM Jr et al. Multisystem inflammatory syndrome in children is driven by zonulin-dependent loss of gut mucosal barrier. J Clin Invest. 2021;131:e149633.
46. Kwak SG, Kim JH. Central limit theorem: the cornerstone of modern statistics. Korean J Anesthesiol. 2017;70:144–156.
47. Bousfiha A et al. The 2022 update of IUIS phenotypical classification for human inborn errors of immunity. J Clin Immunol. 2022; 42:1508–1520.
48. Goswami C, Chattopadhyay A, Chuang EY. Rare variants: data types and analysis strategies. Ann Transl Med. 2021;9:961–964.
49. Rentzsch P, Schubach M, Shendure J, Kircher M. CADD-Splice-improving genome-wide variant effect prediction using deep learning-derived splice scores. Genome Med. 2021;13:31–42.
50. Szymanski CJ, Humphries WHT, Payne CK. Single particle tracking as a method to resolve differences in highly colocalized proteins. Analyst. 2011;136:3527–3533.
51. Talbert ML, Malicdan MCV, Introne WJ. Chediak-Higashi syndrome. Curr Opin Hematol. 2023;30:144–151.
52. Kaplan J, De Domenico I, Ward DM. Chediak-Higashi syndrome. Curr Opin Hematol. 2008;15:22–29.
53. Wong YC, Kim S, Peng W, Krainc D. Regulation and function of mitochondria-lysosome membrane contact sites in cellular homeostasis. Trends Cell Biol. 2019;29:500–513.
54. Mills EL, Kelly B, O'Neill LAJ. Mitochondria are the powerhouses of immunity. Nat Immunol. 2017;18:488–498.
55. Wang Y, Li N, Zhang X, Horng T. Mitochondrial metabolism regulates macrophage biology. J Biol Chem. 2021;297: 100904–100914.
56. Feldstein LR Jr et al.; Overcoming COVID-19 Investigators. Characteristics and outcomes of US children and adolescents with multisystem inflammatory syndrome in children (MIS-C) compared with severe acute COVID-19. JAMA. 2021;325:1074–1087.
57. Song M, Graubard BI, Rabkin CS, Engels EA. Neutrophil-to-lymphocyte ratio and mortality in the United States general population. Sci Rep. 2021;11:464–472.
58. Khan S et al. SARS-CoV-2 spike protein induces inflammation via TLR2-dependent activation of the NF-kappaB pathway. Elife. 2021;10:e68563.
59. Tyrkalska SD et al. The Spike protein of SARS-CoV-2 signals via Tlr2 in zebrafish. Dev Comp Immunol. 2023;140:104626–104633.
60. Zhao Y et al. SARS-CoV-2 spike protein interacts with and activates TLR41. Cell Res. 2021;31:818–820.
61. Fontes-Dantas FL et al. SARS-CoV-2 Spike protein induces TLR4-mediated long-term cognitive dysfunction recapitulating post-COVID-19 syndrome in mice. Cell Rep. 2023;42:112189–112209.
62. Samsudin F et al. SARS-CoV-2 spike protein as a bacterial lipopolysaccharide delivery system in an overzealous inflammatory cascade. J Mol Cell Biol. 2023;14:mjac058.
63. Risma KA, Marsh RA. Hemophagocytic lymphohistiocytosis: clinical presentations and diagnosis. J Allergy Clin Immunol Pract. 2019;7:824–832.
64. Bloch C et al.; French HLH Study Group. Severe adult hemophagocytic lymphohistiocytosis (HLHa) correlates with HLH-related gene variants. J Allergy Clin Immunol. 2024;153:256–264.
65. Vagrecha A et al. Hemophagocytic lymphohistiocytosis gene variants in multisystem inflammatory syndrome in children. Biology (Basel). 2022;11:417–425.
66. Needle RF, Russell RS. Immunity debt, a gap in learning, or immune dysfunction? Viral Immunol. 2023;36:1–2.
67. Billard MN, Bont LJ. Quantifying the RSV immunity debt following COVID-19: a public health matter. Lancet Infect Dis. 2023;23:3–5.
68. Chen C et al. Global prevalence of post-coronavirus disease 2019 (COVID-19) condition or long COVID: a meta-analysis and systematic review. J Infect Dis. 2022;226:1593–1607.
69. Davis HE, McCorkell L, Vogel JM, Topol EJ. Long COVID: major findings, mechanisms and recommendations. Nat Rev Microbiol. 2023;21:133–146.
70. Cheong JG et al. Epigenetic memory of coronavirus infection in innate immune cells and their progenitors. Cell. 2023;186:3882–3902.e4.

 The Journal of Immunology, 2025, 214, 373–383
https://doi.org/10.1093/jimmun/vkaf006 Research Article